A numerical model of the evolution of ocean sulfate and sedimentary sulfur during the last 800 million years

Louis M. François and Jean-Claude Gérard

Institut d'Astrophysique, Université de Liège, Avenue de Cointe, 5, B-4200 Cointe-Liège, Belgium

Abstract—A reservoir model describing the time evolution of the sedimentary cycle of sulfur over the past 800 my has been developed. As a first approximation, the ocean sulfate concentration is assumed to be time-independent. With this assumption, the model is integrated backward in time and a new initialization procedure is derived in order to calculate the present state of the system which must be compatible with both observational data and model equations. The effects of a variation of the present state of the cycle on its past evolution are investigated. It is found that, when the present gypsum reservoir content is too low or when the weathering rate constants are too high, no acceptable solution can be obtained for the evolution of the cycle, since one reservoir is forced to depletion. The sensitivity of the model to the mean isotopic composition of the sedimentary system and to the fractionation factor during pyrite formation is also studied.

Moreover, a model with time-dependent ocean sulfate concentration was developed. The existence of an acceptable solution appears to be linked to the steady state hypothesis for ocean sulfate, since a model with no acceptable steady state solution may be integrated until $t = -800$ my without any problem of reservoir depletion when the time-dependent equations are used.

A tentative evolution of the ocean sulfate concentration is calculated. It is shown that this concentration is negatively correlated to the $\delta^{34}S$ of seawater sulfate. The carbon cycle is modelled in order to compare the calculated $\delta^{13}C$ of carbonate deposits to the observational data.
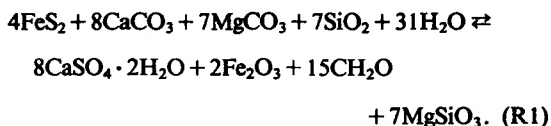
INTRODUCTION

IN THE PAST, much effort was devoted to the description of the present state of the geochemical cycles. Recently, time-dependent numerical models of the evolution of the ocean-atmosphere-crust system were developed by several groups. In this paper, we propose an analysis of several mathematical problems linked to the modeling of the long-term evolution of the Phanerozoic sulfur cycle. The knowledge of this geochemical cycle is important for various reasons. From an ecological point of view, the sulfur cycle is tied to important biological processes such as sulfate reduction by bacteria. The sulfur cycle is also essential to improve our knowledge of the long-term evolution of the atmospheric composition. The evolution of atmospheric oxygen is closely linked to the evolution of the sulfur cycle since pyrite burial and pyrite weathering are respectively a source and a sink for atmospheric oxygen. Moreover, the mixing ratio of atmospheric carbon dioxide (and consequently the climate) depends on the alkalinity of seawater and thus on ocean sulfate concentration. Therefore, despite the low atmospheric abundance of sulfur compounds, a time-dependent model of the geochemical sulfur cycle is necessary to describe the long-term evolution of atmospheric composition and climate.

HOLSER and KAPLAN (1966) published observational data on the Phanerozoic evolution of $\delta^{34}S$ of sulfates in evaporite deposits showing important time variations. Since evaporites are formed from seawater evaporation (a process which does not appreciably alter the isotopic composition of sulfates), their $\delta^{34}S$ reflect the isotopic abundance of seawater sulfur at the time of deposition. Thus, it is clear that the sulfur isotopic composition of seawater has greatly varied throughout the Phanerozoic. REES (1970) developed a model in which the ocean sulfate content is in steady state and showed that this steady state assumption is compatible with the time variations of $\delta^{34}S$ of seawater. He argued that the $\delta^{34}S$ of seawater is governed by the relative magnitude of the deposition rate of sulfur in evaporite formations to the deposition rate of pyrite (light) sulfur in the sediments. HOLLAND (1973) has extended the model of Rees to the general case where the seawater sulfate concentration is allowed to vary. He derived a relationship linking the time variation of $\delta^{34}S$ of seawater to the isotopic composition of river water and to the ocean sulfur input and output fluxes.

GARRELS and PERRY (1974) presented steady state models describing the present state of the geochemical cycles for the major elements. They also studied a system in which the atmosphere and ocean have a constant composition. They proposed the following global chemical reaction:

$$4FeS_2 + 8CaCO_3 + 7MgCO_3 + 7SiO_2 + 31H_2O \rightleftarrows$$

$$8CaSO_4 \cdot 2H_2O + 2Fe_2O_3 + 15CH_2O$$

$$+ 7MgSiO_3. \quad (R1)$$

This chemical reaction, which can evolve either to the right or to the left, represents the global exchanges between the main sedimentary reservoirs of the crust. The atmosphere and oceans are only "transit" reservoirs and do not affect the contents of the sedimentary reservoirs.

SCHIDLOWSKI *et al.* (1977) developed a time-dependent model of the sulfur and carbon cycles based on the available data for the history of seawater $\delta^{34}S$ and

δ^{13}C. They studied the evolution of the sulfate-bound oxygen (crust + ocean) and calculated the Phanerozoic evolution of the reservoir of total oxygen (atmospheric + sedimentary) which is the stoichiometric equivalent of sedimentary organic carbon reservoir. SCHIDLOWSKI and JUNGE (1981) repeated a similar calculation based on new mean values, by VEIZER *et al.* (1980), of δ^{13}C for the carbonates deposited during the different geological periods (these δ^{13}C have also been revised by VEIZER, 1983).

CLAYPOOL *et al.* (1980) reported revised values for the Phanerozoic evolution of δ^{34}S in evaporite deposits. The δ^{13}C of VEIZER *et al.* (1980) show a negative correlation with these δ^{34}S values, suggesting that the carbon and sulfur cycles are linked together. VEIZER *et al.* (1980) proposed that the linking process was the chemical reaction (R1). Using the same assumption, GARRELS and LERMAN (1981) (hereafter referred to as GL81) developed a time-dependent reservoir model of the Phanerozoic cycles of carbon and sulfur. Under the assumption that the ocean sulfate is in steady state they calculated the evolution of the sizes and mean isotopic composition of the sedimentary pyrite and gypsum reservoirs. As a result of (R1), pyrite and organic carbon (CH_2O) deposition rates must be negatively correlated. However, in modern sediments, the abundance of pyrite and organic carbon are proportional, a relationship which would suggest a positive correlation. This apparent paradox was explained by BERNER and RAISWELL (1983) (hereafter referred to as BR): the location (marine or continental) of organic carbon and pyrite deposition changes from one period to another, so that the rates of these depositions can be negatively correlated since continental sediments contain less pyrite than marine sediments. GARRELS and LERMAN (1984) (hereafter referred to as GL84) revised the numerical method of GL81. They observed, indeed, that the initial version of their model was not reversible in time.

In the GL81 and GL84 models, the time evolution of the sulfur cycle is calculated backward from the present state of the cycle. However it is difficult to assign correct values to present contents and mean δ^{34}S of total reduced and oxidised sulfur sedimentary reservoirs. Thus, it is of interest to investigate the effects of a variation in the present state of the sulfur cycle on its calculated past evolution.

Such an investigation, based on a new initialization procedure, is presented in this paper. Two important aspects are examined. First, there exists a domain of present conditions for which the model has no acceptable solution, as a result of an incompatibility between the present reservoir sizes and the observational δ^{34}S values of the evaporite deposits. The boundary of this domain is studied. Secondly, the sensitivity of the model to the mean δ^{34}S of the sedimentary system and to the fractionation factor during pyrite deposition is analysed. The validity of the model will be tested in two ways: the results will be compared with previous models and the integration will be reverted in time to ensure numerical stability. Since, in Garrels and Lerman's models, the ocean sulfate reservoir is assumed to be in steady state, we propose to analyse this approximation. As in the GL81's paper, the carbon cyc' is modelled in order to compare the calculated δ^{13}C or carbonate deposits to the mean observational data of VEIZER *et al.* (1980).

THE MODEL

The sulfur and carbon systems are both divided into three reservoirs. The first one represents the element in the ocean-atmosphere system and the other two the element in the crust in reduced and oxidised states. In Fig. 1, a subscript is assigned to each reservoir. S_1, S_2 and C_5, C_6 are respectively the contents of reduced and oxidised sedimentary sulfur and reduced and oxidised sedimentary carbon reservoirs. S_3 and C_4 are the sulfur and carbon contents of the ocean-atmosphere system.

The isotopic composition of reservoir i is represented by r_i or δ_i, where r_i is the ratio of the quantity of heavy to the quantity of light isotope in the reservoir and δ_i, expressed in per mil, is related to r_i by

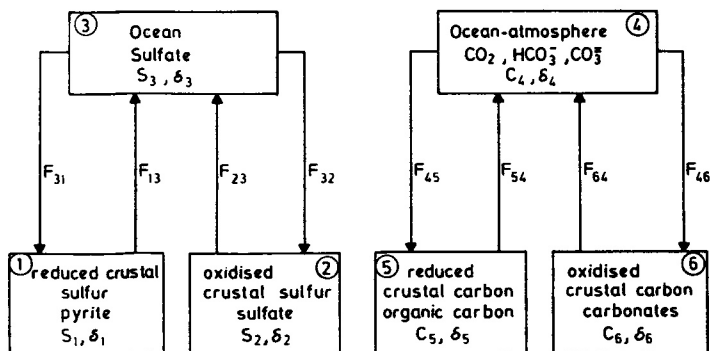$$\delta_i = \left(\frac{r_i}{r_{st}} - 1\right) \times 10^3 \ (\permil), \qquad (1)$$

FIG. 1. Sedimentary cycles of sulfur and carbon as modelled in the numerical simulations.

with r_{st} the ratio of the abundance of heavy to the abundance of light isotope in the standard for the measure of $\delta^{34}S$ ($i = 1, 2, 3$) or $\delta^{13}C$ ($i = 4, 5, 6$). With this definition, δ_i is the mean value of $\delta^{34}S$ or $\delta^{13}C$ in the reservoir.

1. Sulfur

Reduced sedimentary sulfur is composed mainly of pyrite (FeS_2) which is formed by bacterial sulfate reduction in seafloor sediments. During this process, an isotopic fractionation occurs so that the pyrite is isotopically lighter than the sulfate from which it originates. In other words, if, at a given time, the sulfate in the ocean has an isotopic composition δ_3, the pyrite which forms in the sediments has the composition $\delta_S^{(1)} = \delta_3 + \alpha_S^{(1)}$, where $\alpha_S^{(1)}$ is a negative number. In the model, this fractionation factor $\alpha_S^{(1)}$ is assumed to be time-independent and equal to $-35‰$. This value, also adopted by GL81 and GL84, is a mean of different fractionation factors showing substantial discrepancies (CLAYPOOL et al., 1980). The flux of pyrite deposition is labelled F_{31}.

The reservoir of oxidised sedimentary sulfur is composed of sulfate minerals (gypsum and anhydrite) which are mostly deposited during evaporite formation (F_{32}). This deposition flux is accompanied by a fractionation process: the sulfate in newly deposited evaporites is heavier than seawater sulfate. Thus the fractionation factor $\alpha_S^{(2)}$ for sulfate deposition is positive. In the model, its value is $1.5‰$, not very different from the $1.65‰$ value of CLAYPOOL et al. (1980), it is also assumed time-independent.

F_{13} and F_{23} are weathering fluxes which feed the ocean sulfate reservoir. They are assumed to be proportional to the sizes of pyrite and gypsum reservoirs, i.e.

$$F_{13} = k_{13}S_1 \qquad (2)$$

$$F_{23} = k_{23}S_2. \qquad (2')$$

With these assumptions, it is possible to derive three relations describing the time evolution of δ_1, δ_2 and δ_3. Using a method similar to HOLLAND (1973), we write from the definition of r_3:

$$\frac{dr_3}{dt} = \frac{d}{dt}\left(\frac{^{34}S_3}{^{32}S_3}\right) = \frac{1}{^{32}S_3}\left(\frac{d^{34}S_3}{dt} - r_3\frac{d^{32}S_3}{dt}\right), \qquad (3)$$

where $^{32}S_3$ and $^{34}S_3$ are the numbers of moles of ^{32}S and ^{34}S in ocean water. Let $r_S^{(1)}$ be the $^{34}S/^{32}S$ ratio in pyrite formed by sulfate reduction in seafloor sediments and $r_S^{(2)}$ the same ratio for sulfate formed during evaporite deposition, then

$$\frac{d^{34}S_3}{dt} = \frac{r_1}{1+r_1}F_{13} + \frac{r_2}{1+r_2}F_{23} - \frac{r_S^{(1)}}{1+r_S^{(1)}}F_{31} - \frac{r_S^{(2)}}{1+r_S^{(2)}}F_{32} \qquad (4)$$

$$\frac{d^{32}S_3}{dt} = \frac{1}{1+r_1}F_{13} + \frac{1}{1+r_2}F_{23} - \frac{1}{1+r_S^{(1)}}F_{31} - \frac{1}{1+r_S^{(2)}}F_{32}. \qquad (4')$$

Introducing these values of $d^{34}S_3/dt$ and $d^{32}S_3/dt$ in (3) and noting that $^{32}S_3 = S_3/(1 + r_3)$, it comes:

$$\frac{S_3}{1+r_3}\frac{dr_3}{dt} = \frac{r_1-r_3}{1+r_1}F_{13} + \frac{r_2-r_3}{1+r_2}F_{23}$$

$$+ \frac{r_3-r_S^{(1)}}{1+r_S^{(1)}}F_{31} + \frac{r_3-r_S^{(2)}}{1+r_S^{(2)}}F_{32}. \qquad (5)$$

The time evolution of r_1 and r_2 may be obtained in a similar fashion:

$$\frac{S_1}{1+r_1}\frac{dr_1}{dt} = \frac{r_S^{(1)}-r_1}{1+r_S^{(1)}}F_{31} \qquad (6)$$

$$\frac{S_2}{1+r_2}\frac{dr_2}{dt} = \frac{r_S^{(2)}-r_2}{1+r_S^{(2)}}F_{32}. \qquad (6')$$

Making use of (1), noting that, for usual values of δ,

$$\frac{\delta}{10^3} \ll \frac{1}{r_{st}} + 1 \qquad (7)$$

and since $\delta_S^{(1)} = \delta_3 + \alpha_S^{(1)}$ and $\delta_S^{(2)} = \delta_3 + \alpha_S^{(2)}$, it comes

$$S_1\frac{d\delta_1}{dt} = (\delta_3 + \alpha_S^{(1)} - \delta_1)F_{31} \qquad (8)$$

$$S_2\frac{d\delta_2}{dt} = (\delta_3 + \alpha_S^{(2)} - \delta_2)F_{32} \qquad (8')$$

$$S_3\frac{d\delta_3}{dt} = (\delta_1 - \delta_3)F_{13} + (\delta_2 - \delta_3)F_{23} - \alpha_S^{(1)}F_{31} - \alpha_S^{(2)}F_{32}. \qquad (8'')$$

This set of three differential equations may be completed with another set of equations describing the time evolution of reservoirs:

$$\frac{dS_1}{dt} = F_{31} - F_{13} \qquad (9)$$

$$\frac{dS_2}{dt} = F_{32} - F_{23} \qquad (9')$$

$$\frac{dS_3}{dt} = (F_{13} + F_{23}) - (F_{31} + F_{32}). \qquad (9'')$$

When relations (8), (8'), and (8'') are added together, it can be shown, using (9), (9') and (9'') that the quantity $\delta_1 S_1 + \delta_2 S_2 + \delta_3 S_3$ is a constant. Since the total sulfur $S_T = S_1 + S_2 + S_3$ is a constant, this means that the mean isotopic composition of the whole system

$$\bar{\delta}_S = \frac{\delta_1 S_1 + \delta_2 S_2 + \delta_3 S_3}{S_1 + S_2 + S_3} \qquad (10)$$

is also a constant, as stated by GL81 and GL84. Note that this statement is true only for the domain of δ values where (7) is valid but if a reservoir was to become abnormally enriched in ^{34}S, relations (5), (6) and (6') would have to be used.

The curve plotted in Fig. 2 is from CLAYPOOL et al. (1980) and shows the $\delta^{34}S$ of sulfates ($\delta_S^{(2)}$) deposited in seafloor sediments of various geological ages. The $\delta^{34}S$ of seawater at the time of deposition is obtained by subtracting $\alpha_S^{(2)}$ from $\delta_S^{(2)}$ value of Fig. 2, so that the function δ_3 and its derivative in relations (8), (8') and (8'') are known.

Since δ_3 is known, Eqns. (2), (2'), (8), (8'), (8''), (9), (9') and (9'') form a system of eight equations with nine unknowns (4 fluxes, 3 reservoir sizes and 2 δ values). One equation is lacking for the solution to be found and it is thus necessary to make a last hypothesis or to constrain the model with other observational data.

As a first approximation, it can be assumed that the sulfate content of the oceans is constant, i.e.

$$\frac{dS_3}{dt} = 0 \quad \text{and} \quad S_3 = S_3(0) \qquad (11)$$

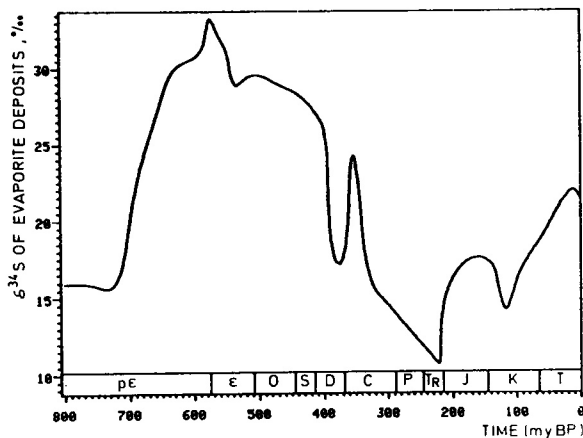where $S_3(0)$ is the present value of S_3. Both GL81 and GL84 made this steady state assumption and used an

FIG. 2. δ^{34}S of sulfate in evaporite deposits of different geological ages as reported by CLAYPOOL et al. (1980).

explicit method to integrate the system of differential equations, with time steps of 10 my. We have integrated the system with an implicit procedure using Gear's method (GEAR, 1971) for systems of differential equations. In order to test this steady state approximation, it is interesting to allow the ocean sulfate content to vary, assuming that the relation among F_{32} and the other variables of the model is known. The simplest is to assume that F_{32} is proportional to S_3, i.e.

$$F_{32} = k_{32}S_3.\qquad(12)$$

A dependence of F_{32} on S_3 of the form

$$F_{32} = k_{32}(S_3 - S_3(eq))\qquad(12')$$

will also be used in the model calculation.

$S_3(eq)$ represents an equilibrium value of S_3 under which the oceans would become globally undersaturated relative to gypsum and anhydrite. In fact, both assumptions are highly speculative since the evaporite deposition rate depends on many factors which are not taken into account in the model, such as climate, extent of intracontinental seas, average concentration of calcium in the ocean, etc.

2. Carbon

Oxidised sedimentary carbon is composed of carbonates (calcite, aragonite, dolomite, etc). Synthesis of organic carbon by organisms is accompanied by a fractionation process for which the mean fractionation factor $\alpha_C^{(5)}$ has a value of -25% (JUNGE et al., 1975), so that the organic carbon deposited on the seafloor is lighter than carbon in ocean (mainly HCO_3^- and CO_3^-) and atmosphere (CO_2). In the model, $\alpha_C^{(5)}$ has a time-independent value of -25%. No fractionation occurs during carbonates deposition. The fluxes of organic carbon and carbonate deposition are labelled F_{45} and F_{46}.

Again, weathering fluxes (F_{54} and F_{64}) are assumed to be proportional to the sizes of organic carbon and carbonates reservoirs:

$$F_{54} = k_{54}C_5\qquad(13)$$

$$F_{64} = k_{64}C_6.\qquad(13')$$

The time evolution of reservoir sizes and isotopic compositions is described by the same relations as for the sulfur cycle, provided $\alpha_C^{(2)}$ be set equal to zero and subscripts 1, 2 and 3 be replaced by 5, 6 and 4 respectively. Thus, one can write:

$$\frac{dC_4}{dt} = (F_{54} + F_{64}) - (F_{45} + F_{46})\qquad(14)$$

$$\frac{dC_5}{dt} = F_{45} - F_{54}\qquad(14')$$

$$\frac{dC_6}{dt} = F_{46} - F_{64}\qquad(14'')$$

$$C_4\frac{d\delta_4}{dt} = (\delta_5 - \delta_4)F_{54} + (\delta_6 - \delta_4)F_{64} - \alpha_C^{(5)}F_{45}\qquad(15)$$

$$C_5\frac{d\delta_5}{dt} = (\delta_4 + \alpha_C^{(5)} - \delta_5)F_{45}\qquad(15')$$

$$C_6\frac{d\delta_6}{dt} = (\delta_4 - \delta_6)F_{46}.\qquad(15'')$$

If it is assumed that the transfers between the reservoirs of the system can be globally represented by the chemical reaction (R1), carbon and sulfur cycles are tied together and the evolution of C_5 is imposed by the stoichiometry of reaction (R1), i.e.

$$\frac{dC_5}{dt} = -\frac{15}{8}\frac{dS_1}{dt}.\qquad(16)$$

For carbon, the steady state hypothesis for the ocean-atmosphere system is more appropriate than for sulfur, since the size of the ocean atmosphere reservoir of carbon is small compared to the sizes of the other reservoirs, so that moderate variations of oceanic and atmospheric carbon cannot appreciably modify the sizes and isotopic compositions of the other reservoirs.

RESULTS AND DISCUSSION

1. Model with steady state ocean sulfate reservoir

Comparison with previous models. We first consider the steady state case for which S_3 is assumed to be time-independent. In their steady state model, both GL81 and GL84 neglected the fractionation process taking place during sulfate deposition. GL81 integrated the differential system backward through time until 600 my BP.

In their set of initial conditions, the three reservoirs at the present time are in steady state with respect to their sizes and isotopic compositions, that is neither sizes nor δ would change if the system was to evolve without being constrained by δ^{34}S of evaporite deposits.

GL84 have revised the numerical method in the model of GL81. They noticed that the GL81 model was not reversible in time. To overcome this problem they developed a "movie model" in which the fluxes are reversed. We have run our model with the same initial conditions and the same rate constants as GL84. The calculated evolutions are similar to those of GL84, the relative deviations being at most of 10%, at the

beginning of the Phanerozoic. This difference is attributed to the fact that GL84 did not include the fractionation factor $\alpha_s^{(2)}$ in their model.

It is however interesting to study the evolution of the sulfur cycle with initial conditions close to those of GL81, in view of the uncertainties on the present system. Thus, we have tried to integrate backward our system of equations with the initial conditions of GL81. However, the integration stops at 370 my BP where S_2 tends to become negative. The problem is tied to the sharp variation of δ_3 during Carboniferous time (see Fig. 2). Thus, an apparent disagreement exists between our model and that of GL81, the latter being integrable through whole Phanerozoic time. However, when our equations are integrated forward with initial conditions at $t = 600$ my BP equal to the values obtained by GL81 for that time, the integration is pursued until $t = 0$, at which time the results do not differ markedly from GL81's initial conditions.

Thus, we may conclude that, when the equations are integrated backward, two domains of initial conditions appear: one for which integration is stopped and another for which integration is pursued throughout the Phanerozoic. In what follows, a model which cannot be integrated until $t = -800$ my due to a reservoir depletion will be said unintegrable. The word "integrability" will be used with this particular meaning and will not refer to its common mathematical significance. For initial conditions not too far from GL81's, the model is very sensitive to the initial values and probably to numerical method (as mentioned earlier, GL81 integrated the system step by step using an explicit method). In this region of high sensitivity, it is interesting to test the time reversibility of our model. Therefore, the model just described (obtained by a forward integration from the conditions of GL81 at $t = -600$ my) has been integrated backward, starting with the calculated present conditions. Between 0 and 300 my, the results of the forward and backward integrations are very close, since they do not differ by more than 0.01%. Beyond the $\delta^{34}S$ peak at 350 my, the discrepancy is somewhat larger but it never exceeds 1.5%. Consequently, it is concluded that the problem of reversibility in time does not arise in our model. The lack of integrability obtained for a backward integration from the initial conditions of GL81 is not simply numerical but denotes an incompatibility between these initial conditions and the recorded $\delta^{34}S$ of evaporites.

Using the steady state model of GL81, BR have calculated the time evolution of the pyrite deposition rate F_{31} with present values of pyrite and gypsum reservoir contents higher than for the GL81 model. We have also computed the same flux F_{31} using our system of equations (backward integration) with the initial conditions of BR. The results are presented in Fig. 3. A good agreement is obtained with BR results: general features are the same, both curves showing an obvious positive correlation with $\delta^{34}S$ of evaporite deposits (Fig. 2). The only differences between the two curves are
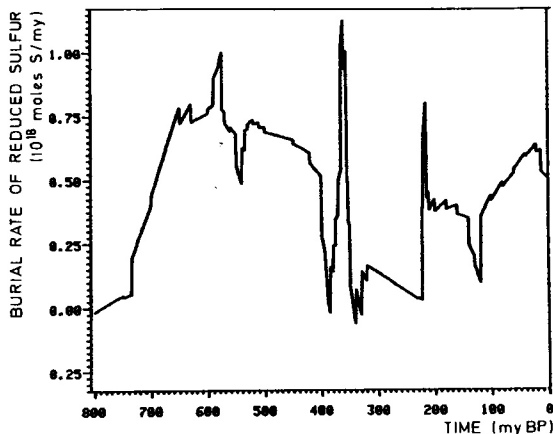

FIG. 3. Burial rate of reduced sulfur (F_{31}) as a function of time calculated (using our steady state model) with the following initial conditions for the present time (see text): $S_1(0) = 250 \times 10^{18}$ moles S, $S_2(0) = 250 \times 10^{18}$ moles S, $\delta_1(0) = -16‰$, $\delta_2(0) = 19‰$, $F_{31}(0) = 0.5 \times 10^{18}$ moles S/my, $F_{32}(0) = 1.0 \times 10^{18}$ moles S/my. The constant value of ocean sulfate reservoir content is 38×10^{18} moles S and the weathering coefficients are $k_{13} = 0.189 \times 10^{-2}$ my^{-1} and $k_{23} = 0.41 \times 10^{-2}$ my^{-1}.

the peak values at about 220 my BP and 360 my BP. In the BR model, these peak values of F_{31} are slightly lower than ours. However this disagreement is possibly due to different time resolutions of the models: the curve of Fig. 3 has been plotted with a time resolution of 1 my whereas BR show only 30 points between 0 and 700 my BP. Another striking feature in Fig. 3 is that, for some short epochs between 300 and 400 my BP, F_{31} takes negative values. Especially, sharply negative values between 391 and 394 my BP have been removed from the curve. However this situation is not really troublesome since negative results appear for very short time intervals and are due to local values of δ_3 and $d\delta_3/dt$ on which uncertainties are important (CLAYPOOL et al., 1980).

In order to test the validity of their model, GL81 calculated the $\delta_{13}C$ values of carbonates deposited at different geological ages with the assumption that carbon and sulfur cycles are linked together through the stoichiometry of reaction R1, i.e. the time evolution of organic carbon reservoir is given by Eqn. (16). The same calculations were repeated with the results of the model presented in Fig. 3. The present state of the carbon cycle was assumed to be the same as in the GL81's model. Mean values of $\delta^{13}C$ for the geological periods have been computed, so that they can be compared with means of observational data reported by VEIZER et al. (1980). The results are given in Table 1. The same general trends are observed between data and model results in this sense that $\delta^{13}C$ are negatively correlated with $\delta^{34}S$. However some substantial differences exist between the two mean values for most geological periods. For example, the calculated mean $\delta^{13}C$ is too low for Tertiary, Cretaceous and Permian. The same was true in the GL81 model as it is obvious from

Table 1. Comparison between observational $\delta^{13}C$ reported by Veizer et al. (1980) and $\delta^{13}C$ calculated from steady state and S_3 time dependent models for the sulfur cycle.

Period	Time before present (my)	$\delta^{13}C$ values from Veizer et al.(1980)	$\delta^{13}C$ values calculated from the fixed ocean sulfate model of fig.3	$\delta^{13}C$ values calculated from the S_3 time-dependent model of fig.7
Tertiary	0-65	0.59	0.17	0.12
Cretaceous	65-143	1.16	0.80	0.64
Jurassic	143-212	0.48	0.72	0.52
Triassic	212-247	0.92	1.23	0.90
Permian	247-289	2.00	1.57	1.43
Carboniferous	289-367	0.35	1.07	1.05
Devonian	367-416	0.21	1.03	1.01
Silurian	416-446	-0.15	-0.08	0.07
Ordovician	446-509	-0.79	-0.27	-0.13
Cambrian	509-575	-0.57	-0.28	-0.29

their Fig. 4. This point will be further examined in the discussion of the S_3 time-dependent model.

Integrability of the equations. Neither GL81 nor GL84 did justify their initial conditions. There is no obvious reason for all the present reservoirs to be in steady state with respect to both sizes and isotopic compositions. A new initialization method for sulfur is presented in the Appendix. It enables us to fix only two independent parameters: the present pyrite reservoir content $S_1(0)$ and the present total weathering flux F_{tot}. The other initial values as well as the rate constants k_{13} and k_{23} are implicitly calculated. In the following text, the terms "initialization procedure" will refer specifically to this new method. The initialization procedure has been used for a set of models with present values of S_1 varying from 100×10^{18} moles to 500×10^{18} moles and present total weathering flux F_{tot} in the range 1.0×10^{18} moles/my to 3.5×10^{18} moles/my. As guessed earlier, two domains of S_1 and F_{tot} values appeared: one where the integration can be performed until 800 my BP and another where the integration is stopped because either S_1 or S_2 reservoir is depleted. An approximate boundary between the two domains is represented in Fig. 4 (standard case). Integrability occurs for high present values of S_1 or low present weathering fluxes F_{tot}. $S_1(0)$ and F_{tot} values of GL81's model fall near the boundary between the two domains. This is the reason why, as shown earlier, their model is very sensitive to the initial conditions or numerical method used. On the contrary, both BR and GL84 adopted higher $S_1(0)$ and $S_2(0)$ so that their models are integrable.

In all the integrable models that we have run, the gypsum reservoir content S_2 has a minimum value always located around 425 my BP. Such a minimum has also been obtained by GL84 and by SCHIDLOWSKI et al. (1977), but not by GL81, a fact that suggests a high sensitivity of the time evolution to the initial values of S_1 and S_2. This high sensitivity of the GL81 model is tied to the proximity of their initial conditions to the boundary of the domain of integrability. In fact, our results indicate that in the vicinity of the boundary

between the two domains, the problem of non-integrability arises because S_2 is forced to depletion. In some cases, the problem is linked to the presence of the 425 my minimum, in this sense that, while the backward integration is pursued after 425 my, S_2 continues to decrease until depletion. In some other cases, however, the problem is not the consequence of the 425 my minimum. Indeed, this minimum is simply shifted backward in time, but a second S_2 decrease appears between 700 and 800 my BP and the reservoir tends to become depleted.

The lower S_2 values between 700 and 800 my are real, since they are also observed in the integrable models, i.e. the S_2 evolution consists of a minimum located at ~425 my and a maximum at ~725 my. Near the boundary between the domains of integrability, the height of the 725 my maximum is very sensitive to the initial values (note that this is not true far
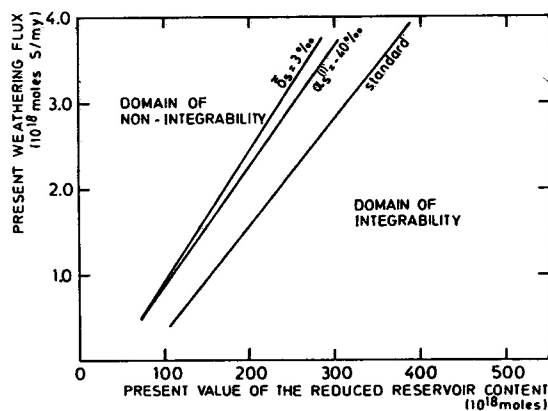

FIG. 4. Domains of integrability and non-integrability for the equations describing the time evolution of the sulfur cycle. A new initialization procedure has been used for which present value of reduced sulfur reservoir content $S_1(0)$ and present weathering flux F_{tot} are the only independent parameters (see text). In the standard model, $\bar{\delta}_s$, the primordial value of $\delta^{34}S$ is assumed to be 0‰ and the fractionation factor during pyrite formation $\alpha_4^{(1)}$ is equal to -35‰. Either $\bar{\delta}_s$ or $\alpha_4^{(1)}$ is varied in the other presented models.

from the boundary). Thus, when $S_2(0)$ is too small, the 725 my maximum is lowered or even vanishes (as in our simulation of the GL81 model) and the gypsum reservoir is forced to depletion, preventing any further progress in the integration. With our initialization procedure, higher $S_1(0)$ values correspond to higher total sulfur and hence to higher $S_2(0)$, so that it is safer to integrate the problem with larger $S_1(0)$.

As mentioned before, a higher initial present weathering flux F_{tot} makes the integration more difficult to perform. The reason is that, with the same $S_1(0)$ value, the rate constants k_{13} and k_{23} are greater for high F_{tot}. In this case, the weathering fluxes F_{13} and F_{23} are higher during the whole past evolution. As a result, the extrema of the S_2 curves are more pronounced and the gypsum reservoir becomes more easily depleted.

GL84 adopted a value of 3.17‰ for $\bar{\delta}_s$ instead of 0‰. Thus, it is interesting to study the sensitivity of the integrability to $\bar{\delta}_s$. In the same way, the sensitivity :he fractionation factor $\alpha_s^{(1)}$ must be examined since values slightly different from −35‰ are possible (for example CLAYPOOL et al. (1980) have used $\alpha_s^{(1)}$ = −40‰). In Fig. 4, an approximate boundary between the domains of integrability and non-integrability is displayed for two classes of models, one with $\bar{\delta}_s = 3‰$ and the other with $\alpha_s^{(1)} = −40‰$. As for the standard case, the new initialization procedure was used. The effects of an increase in $\bar{\delta}_s$ or a decrease in $\alpha_s^{(1)}$ are the same. In each case, the boundary between the two domains is shifted to lower $S_1(0)$ values. It is observed that, owing to the initialization procedure, models with the same $S_1(0)$ and F_{tot} have larger $S_2(0)$ and lower rate constants when $\bar{\delta}_s$ is higher or $\alpha_s^{(1)}$ is lower. As discussed earlier, both conditions act in opposition to the S_2 depletion, thus increasing the size of the integrability domain.

The rate constant k_{23} seems critical for the integrability problem. In all the models based on the initialization procedure, it was indeed noticed that the non-integrability arises when k_{23} became larger than roughly

0.9×10^{-2} my^{-1}. The GL81 value $k_{23} = 0.926 \times 10^{-2}$ my^{-1} is very close to this limit (by contrast, note that GL84 adopted a much lower value $k_{23} = 0.5 \times 10^{-2}$ my^{-1}). The question which comes to mind is the following: can a non-integrable model become integrable after a single decrease in k_{23}? In order to answer this question, a model with initial conditions close to those of GL81 (except that $S_1(0) = 200 \times 10^{18}$ moles) has been run. The values of the rate constants were k_{13} = 0.25 my^{-1} and $k_{23} = 0.9$ my^{-1}. The integration was stopped at $t = 380$ my BP. If k_{23} is decreased to the value $k_{23} = 0.5$ my^{-1}, the model is still non-integrable and a further decrease until $k_{23} = 0.3$ my^{-1} is necessary to recover the integrability.

In conclusion, one may say that two parameters basically control the integrability: the present gypsum reservoir content $S_2(0)$ and the rate constant k_{23}. The problem may be summarized as follows: a too low $S_2(0)$ or a too high k_{23} are incompatible with the recorded evolution of the isotopic composition of seawater sulfate. However, low $S_2(0)$ or high k_{23} values are not necessarily to be refuted since it is not sure that the incompatibility is real or if it is a mere consequence of some model hypothesis. For example, the possible dependence of the rate constants on climate (WALKER et al., 1981) and on the presence or the absence of land plants has not been taken into account. If, due to these factors, the rate constants k_{13} and k_{23} were lower in the past, the domain of integrability would be enlarged. Another important assumption is that the ocean sulfate is in steady state. As we shall see later, the abandon of this hypothesis is also a possible way to make low $S_2(0)$ or high k_{23} values compatible with the isotopic data.

Sensitivity analysis. In this section, the models which were run to study the problem of integrability will be used to describe the sensitivity of the time evolutions of S_1, S_2, δ_1 and δ_2 to a variation in the basic parameters $S_1(0)$, F_{tot}, $\bar{\delta}_s$ and $\alpha_s^{(1)}$. For this purpose, several models have been selected for which the various parameters are listed in Table 2.

Table 2. Values of the various parameters in the models labelled 1 to 8 in figures 5 and 6. The calculated values of the rate constants are displayed. The initialization procedure was used in each case except for model 8 where the initial conditions and the rate constants were taken from model 6.

Model Number	Present content $S_1(0)$ of reduced sulfur reservoir (10^{18} moles)	Present total weathering flux F_{tot} (10^{18} moles my^{-1})	Primordial $\delta^{34}S$ $\bar{\delta}_s$ (‰)	Fractionation factor $\alpha_s^{(1)}$ (‰)	Rate constants	
					k_{13} (10^{-2} my^{-1})	k_{23} (10^{-2} my^{-1})
1	350	1.5	0	−35	0.136	0.469
2	200	1.5	0	−35	0.233	0.876
3	350	3.0	0	−35	0.264	0.857
4	200	1.5	3	−35	0.232	0.556
5	350	3.0	3	−35	0.264	0.571
6	250	2.0	0	−35	0.247	0.866
7	250	2.0	0	−40	0.216	0.654
8	250	2.0	0	−40	0.247	0.866

Sensitivity to $S_I(0)$ and F_{tot}. The sensitivity to $S_I(0)$ and F_{tot} is illustrated in Fig. 5. Owing to the initialization procedure, an increase in $S_I(0)$ corresponds to an increase in total sulfur and, thus, to an increase in $S_2(0)$. The effect on the evolution is simply to shift the S_1 and S_2 curves to higher values. The evolutions of δ_1 and δ_2 are not very dependent on the initial pyrite reservoir content. For δ_1, the maximum scatter between model 1 and 2 is observed for $t = 0$ and $t = -800$ my, the differences between the two curves being of the order of 1‰. For δ_2, the magnitude of the difference is somewhat higher (2–3‰) but the present value seems better known. The comparison between model 1 and 3 gives an idea of the sensitivity to the total present weathering flux F_{tot}. As already mentioned during the discussion of integrability, a variation of F_{tot} leads to a variation in the rate constants k_{13} and k_{23}. Consequently, an increase in F_{tot} results in the amplification of the time fluctuations in the reservoirs contents. As shown in Fig. 5a–b, when F_{tot} is varied from 1.5×10^{18} moles/my to 3.0×10^{18} moles/my, S_1 and S_2 show relative variations of at most 10%. From Fig. 5c–d, it is seen that model 3 is very similar to model 2, as far as the isotopic compositions are concerned. Thus, an increase of F_{tot} has the same effect on δ_1 and δ_2 than a decrease of $S_1(0)$. It is also interesting to mention that, in all the integrable models which were performed, present δ_1 values range between -14.8‰ and -13‰ and present δ_2 are always very close to 18‰. It seems therefore that present δ_1 and δ_2 are well-known quantities. To ensure that the results are not too much dependent on the mean $\delta^{34}S$ of river water (δ_R), model 1 has been re-run with $\delta_R = 6$‰ instead of 8‰ in the initialization procedure. No large differences were observed for the evolutions of the reservoir sizes or isotopic compositions. S_1 did not deviate from model 1

results by more than ~ 1%, while the S_2 curve was shifted to higher contents by only an amount of 10×10^{18} moles (~ 5%) due to a small difference in its initial value. Similarly, the deviations for δ_1 and δ_2 were not important, since, at most, they were of the order of ~ 0.5‰.

Sensitivity to $\bar{\delta}_s$. The sensitivity to $\bar{\delta}_S$ is illustrated in Fig. 6a–b. In models 4 and 5, $\bar{\delta}_s$ has been increased to 3‰ and may be compared with models 2 and 3. It is clear that the time evolution of S_1 depends very weakly on $\bar{\delta}_s$. Many models with $\bar{\delta}_s = 3$‰ were run to study the problem of integrability. The deviation with the corresponding cases at $\bar{\delta}_s = 0$‰ is never higher than 1 or 2%. When $\bar{\delta}_s$ is increased, it is observed that S_2 becomes higher. That is the result of the initialization procedure, in which the present isotopic composition of river water must remain equal to 8‰ independently of the increase in $\bar{\delta}_s$. Thus, the model starts the integration with a higher S_2 value, and, hence, with higher total sulfur. The effect is similar to the results obtained when $S_1(0)$ is varied, *i.e.* the S_2 curve is globally shifted to higher values. By contrast, the δ_1 and δ_2 evolutions are not greatly affected by a higher $\bar{\delta}_s$ value: they are increased by only a fraction of per mil during the whole history, except in the vicinity of the S_2 minimum (425 my BP) where they are somewhat decreased, probably resulting from the lower values of k_{13} and k_{23} (see the discussion of integrability).

Sensitivity to $\alpha_s^{(1)}$. The sensitivity to $\alpha_s^{(1)}$ has also been examined. One model with $\alpha_s^{(1)} = -40$‰ was chosen and is displayed in Fig. 6c–d (case 7). The comparison of curves 6 and 7 shows that, if the initialization procedure is used, the evolution of S_1 is almost independent of the $\alpha_s^{(1)}$ value. The S_2 curve is again shifted to higher values, when $\alpha_s^{(1)}$ is decreased, as for the models described to study the effect of a change in $\bar{\delta}_s$. The
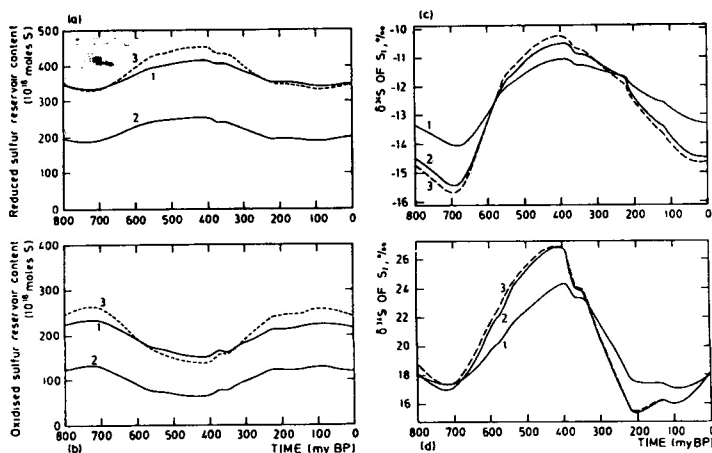

FIG. 5. Influence of the present pyrite reservoir content $S_1(0)$ and of the present total weathering flux F_{tot} on the past evolution of the sulfur cycle. Both the time evolution of the reservoir contents (a, b) and of the isotopic compositions (c, d) are shown. The numbers besides the curves refer to the models in Table 2. The values $\bar{\delta}_S = 0$‰ and $\alpha_s^{(1)} = -35$‰ are adopted. $S_1(0)$ and F_{tot} are as follows: 1: $S_1(0) = 350 \times 10^{18}$ moles, $F_{tot} = 1.5 \times 10^{18}$ moles yr^{-1}; 2: $S_1(0) = 200 \times 10^{18}$ moles, $F_{tot} = 1.5 \times 10^{18}$ moles yr^{-1}; 3: $S_1(0) = 350 \times 10^{18}$ moles, $F_{tot} = 3.0 \times 10^{18}$ moles yr^{-1}.
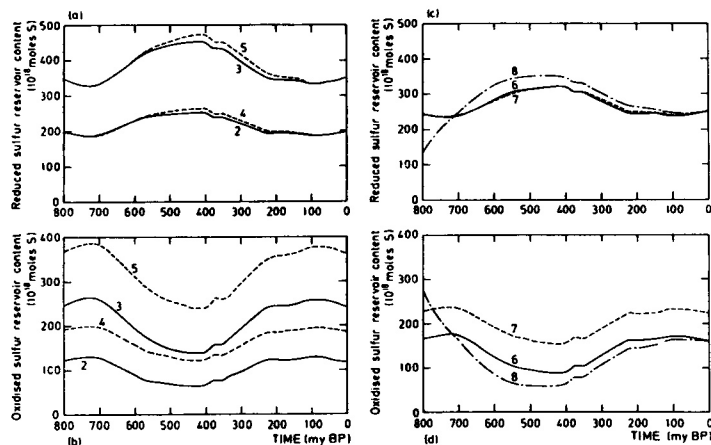
FIG. 6. Sensitivity of the evolution of the reservoir contents to $\bar{\delta}_s$, the primordial value of $\delta^{34}S$, and to $\alpha_s^{(1)}$, the fractionation factor during pyrite formation. The numbers beside the curves refer to the models in Table 2. Models 4 and 5 respectively differ from models 2 and 3 by a higher $\bar{\delta}_S$ value: $\bar{\delta}_S = 3\permil$ instead of $\bar{\delta}_S = 0\permil$. In models 6, 7 and 8 the values $S_1(0) = 250 \times 10^{18}$ moles, $F_{tot} = 2.0 \times 10^{18}$ moles yr^{-1} and $\bar{\delta}_S = 0\permil$ are adopted. For model 6, $\alpha_s^{(1)} = -35\permil$ and for models 7 and 8, $\alpha_s^{(1)} = -40\permil$. In the latter case (8), the initialization procedure (see text) is not used.

evolution of δ_2 is not greatly altered, since it shows at most a $1\permil$ variation. On the contrary, δ_1 is decreased by about $5\permil$, reflecting the $5\permil$ decrease in $\alpha_s^{(1)}$. Case 8 in Fig. 6c–d shows the S_1 and S_2 evolutions obtained for $\alpha_s^{(1)} = -40\permil$, when the initialization procedure is not used, i.e. when the initial conditions (for reservoir contents and isotopic compositions) and rate constants are taken from model 6. It is observed that the sensitivity of S_1 and S_2 is increased. Furthermore, the maximum in the S_2 curve at $t = -725$ my BP has vanished. The evolutions of δ_1 and δ_2 between $t = -800$ my and $t = -500$ my differ radically from the usual evolution: δ_2 becomes negative and δ_1 is forced to positive values. In fact, this indicates a high sensitivity of the model to the initial value of δ_1. When δ_1 is calculated by the initialization method, it is consistent with the other ta of the model. However, when δ_1 is arbitrarily fixed, the consequences on the evolution curves may be dramatic.

2. Model with time-dependent ocean sulfate reservoir

The S_3 time-dependent system has been previously studied by LASAGA et al. (1985). They analysed the sensitivity of a geochemical model of carbon and sulfur cycles to the hypothesis that the ocean sulfate is in steady state. For this purpose, they imposed an arbitrary evolution of seawater sulfate. This approach may be justified when it is intended to study the influence of the steady state hypothesis on the carbon cycle. However, when the purpose is the study of the sulfur cycle itself, Eqns. (12) and (12′) are more useful. Furthermore, the model of LASAGA et al. (1985) is valid only for the last 100 my. In this section, the S_3 time-dependent model will help us to discuss further the problem

of integrability and, thereafter, a tentative evolution of ocean sulfate will be derived.

The S_3 time-dependent system was integrated forward in time for reasons of numerical stability. Consequently, initial conditions were chosen at $t = 800$ my BP and the new initialization procedure was not used. As discussed earlier, the time evolution of δ_1 and δ_2 are relatively well determined, so that their initial values at 800 my BP were imposed:

$$\delta_1(-800) = -14.45\permil$$

$$\delta_2(-800) = 18.50\permil.$$

First, a model based on (12) has been run. The constant coefficient k_{32} was computed from present values of ocean sulfate content ($S_3(0) = 38 \times 10^{18}$ moles) and gypsum deposition rate ($F_{32}(0) = 0.87 \times 10^{18}$ moles/ my). This value for $F_{32}(0)$ somewhat lower than GL81's value, is from BOLIN et al. (1983). Weathering coefficients k_{13} and k_{23} were initially chosen close to GL81's values but were regarded as free parameters. S_1 and S_3 values at $t = -800$ my were also regarded as parameters. $S_2(-800)$ was evaluated from the requirement that $\bar{\delta}_S = 0\permil$. It was observed that varying $S_3(-800)$ had an appreciable effect only on the evolution of the first 50 my which is twice the residence time of sulfate in the ocean. Thus $S_3(-800)$ has been fixed to 50×10^{18} moles, keeping in mind that the results are uncertain between 800 my BP and 750 my BP. Values of $S_1(-800)$, k_{13} and k_{23} were varied in such a way that the present ocean sulfate reservoir content be equal to 38×10^{18} moles and the present $\delta^{34}S$ of river water be close to $8\permil$. (Eqn. (A2)). The optimum run was obtained with $S_1(-800) = 178 \times 10^{18}$ moles, $k_{13} = 0.23 \times 10^{-2}$ my^{-1} and $k_{23} = 0.9 \times 10^{-2}$ my^{-1}. Present state of the system is as follows:

$$S_1(0) = 185.4 \times 10^{18} \text{ moles}$$
$$S_2(0) = 104.6 \times 10^{18} \text{ moles}$$
$$S_3(0) = 38.1 \times 10^{18} \text{ moles}$$
$$\delta_1(0) = -14.45\text{‰}$$
$$\delta_2(0) = 18.28\text{‰}$$
$$F_{31}(0) = 0.445 \times 10^{18} \text{ moles/my}$$
$$F_{32}(0) = 0.873 \times 10^{18} \text{ moles/my}$$
$$\delta_R = 8.07\text{‰}.$$

These values were used as initial conditions for a steady state model integrated backward.

The results are displayed in Fig. 7 where time evolutions of S_1, S_2, δ_1 and δ_2 are represented for the steady state (dashed line) and S_3 time-dependent (solid line) models. The evolutions of the two models are similar between 0 and 350 my BP, but they are radically different for earlier time. Again, for the S_3 time-dependent model, a minimum S_2 value is obtained at about 400 my BP. However, this minimum value does not occur in the steady state case: S_2 continues to decrease beyond 400 my and ultimately reaches zero, so that the problem is not integrable. In other words, a non integrable steady state model becomes integrable when the ocean sulfate concentration is allowed to vary. Furthermore, the main features of the evolution of a S_3 time-dependent model are the same as for integrable steady state models, i.e. S_2 reaches a minimum value about 400

my BP and the evolutions of δ_1 and δ_2 are similar to the steady state evolutions of Fig. 5c–d. As shown for the steady state case, a lower k_{23} value makes the integration easier to perform. To test the integrability, the rate constant k_{23} has been increased ($k_{23} = 1.1 \times 10^{-2}$ my^{-1}) in the time-dependent model. The forward integration was easily performed and yielded a lower present S_2 value. Neither a high k_{23} nor a low $S_2(0)$ favours the integrability of the steady state system. Consequently, the present conditions calculated with $k_{23} = 1.1 \times 10^{-2}$ my^{-1} in the S_3 time-dependent model fall largely in the domain of non-integrability in the steady state case. It is tempting to believe that fluctuations of ocean sulfate can always solve the problem of integrability. This point may be understood as follows. In the steady state case, the non-integrability arises when S_2 is too low to explain the large fluctuations in the ocean isotopic composition as recorded in the evaporite deposits. However, in a S_3 time-dependent model, the integrability is recovered because the ocean sulfate content may decrease in such a way that a similar change in the fluxes may have greater effects on the isotopic composition of seawater.

Assuming that (16) is valid, mean $\delta^{13}C$ values of carbonates of different geological periods have been calculated from the results of the S_3 time-dependent model. These $\delta^{13}C$ values are displayed in Table 1. There is no marked difference with the steady state
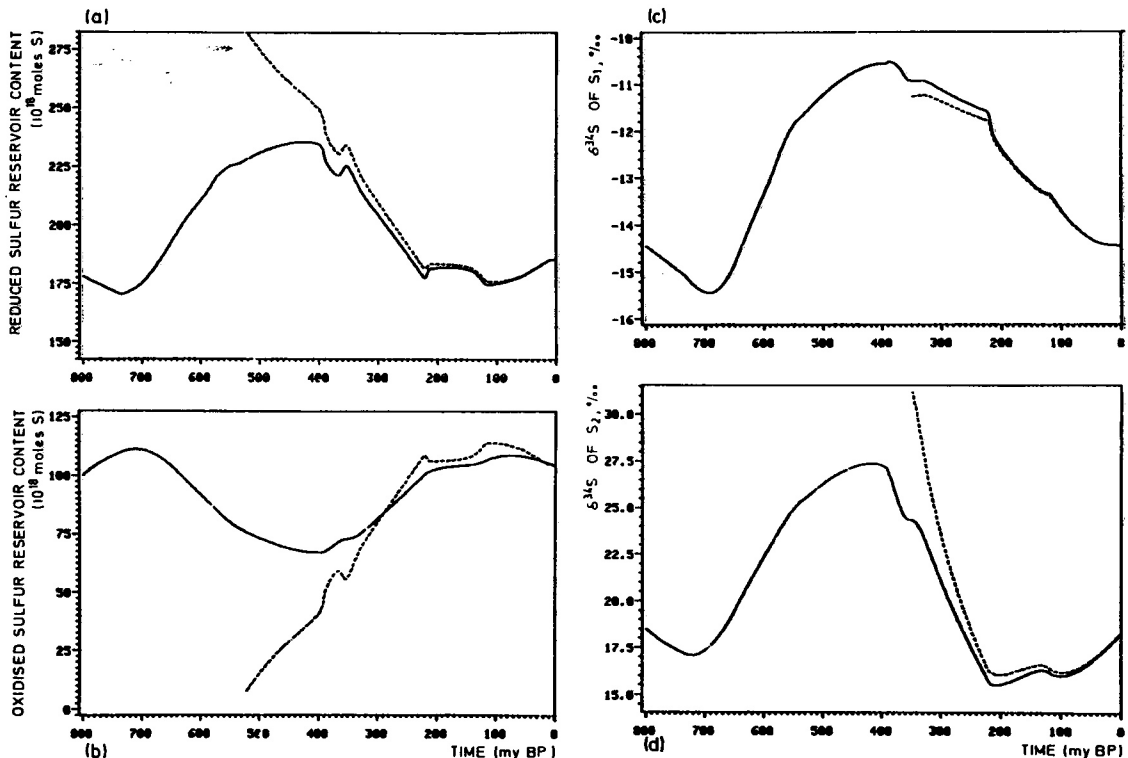

FIG. 7. Time evolution of reduced and oxidised sulfur reservoir contents (a, b) and isotopic compositions (c, d) for a model where the ocean sulfate reservoir is in steady state (dashed line) and another where it is allowed to vary (solid line). Present states of the system are the same for the two models. Weathering coefficients are $k_{13} = 0.23 \times 10^{-2}$ my^{-1} and $k_{23} = 0.9 \times 10^{-2}$ my^{-1}. The integration was stopped in the steady state case since oxidised sulfur reservoir content tended to become negative.

case except that recent $\delta^{13}C$ are somewhat lower. In each case, it is obvious that $\delta^{13}C$ are negatively correlated with $\delta^{34}S$. Observational data show the same negative correlation. Thus, it is clear that when the organic carbon burial rate increases the pyrite burial rate decreases and inversely, this being possibly linked to the location of organic carbon burial, as suggested by BR. However this assertion does not mean that (16) is reliable, *i.e.* it is possible that the fluctuations of the organic carbon burial rate are not entirely compensated but simply damped by the fluctuations of pyrite burial, so that the atmospheric oxygen production rate could vary. One could consider computing the time evolution of this oxygen production rate with a model of the carbon cycle where observational $\delta^{13}C$ are used as input data as it was the case for $\delta^{34}S$ in our model of the sulfur cycle. SCHIDLOWSKI *et al.* (1977) and SCHIDLOWSKI and JUNGE (1981) have performed similar calculations. However, the validity of this method is ot guaranteed when the purpose is the calculation of the evolution of non sulfate-bound oxygen since uncertainties on observational $\delta^{13}C$ are important and actually larger (VEIZER and HOEFS, 1976) than the deviations of observational $\delta^{13}C$ from our calculated values. Another possible reason for which (16) might not be valid is given by LERMAN (1982). If the CO_2 consumed by photosynthesis in reaction R1 is derived from the weathering of $FeCO_3$ instead of $MgCO_3$, then the proportionality factor in Eqn. (16) would be equal to 13/6 instead of 15/8. LERMAN (1982) proposed a more general approach of the problem where the CO_2 source for photosynthesis is the weathering of siderite and dolomite or may even take into account the CO_2 release from the earth's interior by volcanoes.

The results of the S_3 time-dependent model may be used to discuss the history of seawater sulfate. In Fig. 8, the evolution of the ocean sulfate reservoir content is represented for the S_3 time-dependent model which has been previously described (solid line) and for a model in which the gypsum deposition flux is calcu-

lated from Eqn. (12') (dashed line). In the latter case, the parameter $S_3(eq)$ was fixed to 19×10^{18} moles. This arbitrary value was chosen midway between $S_3(eq) = 0$ implicit in Eqn. (12) and the present ocean sulfate content, in order to test the sensitivity of the model to kinetics of SO_4^{2-} removal. Initial conditions at 600 my BP and weathering coefficients are the same for the two models and the requirements that the present ocean sulfate reservoir content and present $\delta^{34}S$ of river water be close to the values

$$S_3(0) = 38 \times 10^{18} \text{ moles}$$

$$\delta_R = 8\%_0$$

are fulfilled in each case. The comparison of Figs. 2 and 8 shows that seawater sulfate concentration is negatively correlated to $\delta^{34}S$, the only effect of setting $S_3(eq)$ to a positive value being to smooth the fluctuations of ocean sulfate. The gypsum deposition flux probably depends on some factors which are not taken into account in Eqns. (12) and (12').

Consequently, the history of ocean sulfate displayed in Fig. 8 remains speculative. However, the negative correlation to $\delta^{34}S$ is obtained with both assumptions on evaporite deposition rate and may be regarded as a significant result. The time variations of S_3 displayed in Fig. 8 are not negligible since departures from the present value of 30% to 40% are obtained. Such departures are small compared to the range of permitted variations between extreme seawater sulfate reservoir content of 2.7×10^{18} moles and 4×10^{20} moles deduced by HOLLAND (1972) from the mineral sequence of evaporites in Phanerozoic sediments.

CONCLUSION

The main purpose of this paper was to analyse the effects of a variation in the present conditions or in various parameters on the past evolution of the sedimentary sulfur cycle.
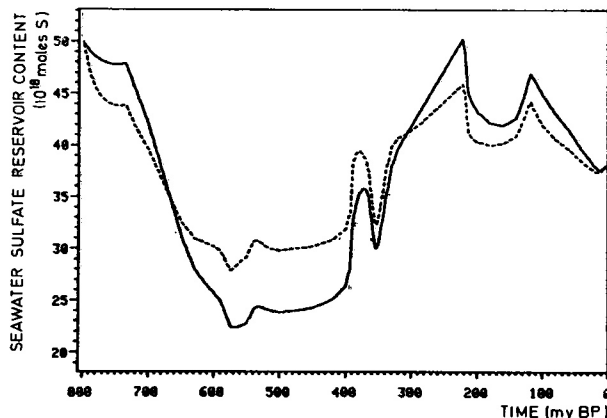

FIG. 8. Evolution of seawater sulfate based on the assumptions that the sulfate deposition flux is related to the ocean sulfate reservoir content through Eqn. (12) (solid line) or (12') (dashed line), with $S_3(eq) = 19 \times 10^{18}$ moles in the latter case. Weathering coefficients are $k_{13} = 0.23 \times 10^{-2}$ my^{-1} and $k_{23} = 0.9 \times 10^{-2}$ my^{-1}.

A model with steady state ocean sulfate has been run. The system of differential equations describing the evolution of the cycle has been integrated backward in time. It is observed that, when the gypsum reservoir content is too low, the integration cannot be pursued until $t = -800$ my. The lack of integrability denotes an incompatibility between the recorded history of the isotopic composition of seawater and a low gypsum reservoir content at the present time. Similarly, a high weathering rate constant k_{23} is not compatible with past $\delta^{34}S$ of ocean sulfate. A new initialization procedure was developed in order to calculate the present state of the cycle. When this method is applied, the size of the domain of integrability may be studied. In general, the integration is favoured by a higher mean $\delta^{34}S$ of the whole sedimentary system ($\bar{\delta}_s$), a more negative fractionation factor $\alpha_s^{(1)}$ during pyrite deposition, higher present reservoir contents or lower fluxes.

The initialization procedure was used to study the sensitivity of the system to the present conditions or to $\bar{\delta}_s$ and $\alpha_s^{(1)}$. It is observed that, when the present reservoir sizes are increased, the evolution curve for this reservoir is simply shifted to higher values. An increase of the present total weathering flux F_{tot} strengthens the fluctuations of the reservoir sizes. A variation of $\bar{\delta}_s$ or $\alpha_s^{(1)}$ has no important consequences on the evolution curves, except for $\alpha_s^{(1)}$ when the initialization procedure is not used. It is also interesting to mention that the evolutions of δ_1 and δ_2—the mean $\delta^{34}S$ of reduced (pyrite) and oxidised (evaporite sulfur) sedimentary reservoir—seem to be well determined except for δ_1 when $\alpha_s^{(1)}$ is varied.

A model with time-dependent ocean sulfate was also developed. It was observed that the problem of integrability vanished, even for low gypsum reservoir contents and a high weathering rate constant k_{23}. Furthermore, the results of this time-dependent model show that the Phanerozoic history of seawater sulfate concentration is negatively correlated to the history of its $\delta^{34}S$. This conclusion is probably only dependent on the assumption that the burial rate of evaporite sulfate increases with the ocean sulfate concentration, as it can be shown with the following arguments. When the ocean sulfate concentration increases, the ratio of the burial rate of evaporite sulfate to the burial rate of pyrite is increased (the pyrite burial rate cannot be increased proportionally to the evaporite sulfate burial rate since, according to BERNER (1984), the rate of bacterial sulfate reduction in seafloor sediments is controlled primarily by the availability and the reactivity of organic matter rather than by the sulfate concentration), so that the mean $\delta^{34}S$ of the sulfur removed from the ocean is higher and seawater sulfate tends to become lighter. Possible departures of 30% to 40% from the present value have been calculated for the evolution of seawater sulfate concentration during the Phanerozoic.

The model presented in this paper is far from complete. Two major approximations have been made. The first one is to consider the sedimentary cycle as closed.

It is clear that, in the real system, metamorphism and volcanism may have affected in an appreciable way the evolution of the sulfur cycle. Secondly, the weathering rate constants k_{13} and k_{23} were assumed constant, although they are dependent on climate (WALKER et al., 1981). The inclusion of this last point would require the calculation of the history of the atmospheric carbon dioxide pressure as well as the exact knowledge of the response of the climate system to an increase in CO_2. An attractive geochemical description of the evolution of the CO_2 cycle has been presented by BERNER et al. (1983) and LASAGA et al. (1985) for the last 100 million years. However, we feel that many aspects of the calculation of the atmospheric CO_2 pressure in such models remain speculative in view of our present knowledge of the geochemical and atmospheric processes involved. In such a case where the system is not well-known, it is clear that sensitivity studies similar to the one presented here may play a complementary role to improve our understanding of the key processes which govern the evolution of the cycles.

REFERENCES

BERNER R. A. (1984) Sedimentary pyrite formation: an update. *Geochim. Cosmochim. Acta* 48, 605–615.

BERNER R. A. and RAISWELL R. (1983) Burial of organic carbon and pyrite sulfur in sediments over Phanerozoic time: a new theory. *Geochim. Cosmochim. Acta* 47, 855–862.

BERNER R. A., LASAGA A. C. and GARRELS R. M. (1983) The carbonate-silicate geochemical cycle and its effect on atmospheric carbon dioxide over the past 100 million years. *Amer. J. Sci.* 283, 641–683.

BOLIN B., ROSSWALL T., FRENEY J. R., IVANOV M. V., RODHE H. and RICHEY J. E. (1983) C, N, P and S cycles: Major reservoirs and fluxes. In *The Major Biogeochemical Cycles and Their Interactions* (eds. B. BOLIN and R. B. COOK), pp. 41–65. Scope Report No 21, Wiley.

CLAYPOOL G. E., HOLSER W. T., KAPLAN I. R., SAKAI H. and ZAK I. (1980) The age curves of sulfur and oxygen isotopes in marine sulfate and their mutual interpretation. *Chem. Geol.* 28, 199–260.

DEINES P. and GOLD D. P. (1973) The isotopic composition of carbonatite and kimberlite carbonates and their bearing on the isotopic composition of deep-seated carbon. *Geochim. Cosmochim. Acta* 37, 1709–1733.

GARRELS R. M. and PERRY E. A. (1974) Cycling of carbon, sulfur and oxygen through geologic time. In *The Sea*, vol. 5, (ed. E. D. GOLDBERG), pp. 303–336. Wiley.

GARRELS R. M. and LERMAN A. (1981) Phanerozoic cycles of sedimentary carbon and sulfur. *Proc. Natl. Acad. Sci. USA* 78, 4652–4656.

GARRELS R. M. and LERMAN A. (1984) Coupling of the sedimentary sulfur and carbon cycles—an improved model. *Amer. J. Sci.* 284, 989–1007.

GEAR C. W. (1971) *Numerical Initial Value Problems in Ordinary Differential Equations.* Prentice-Hall, Englewood Cliffs, N.J.

HOLLAND H. D. (1972) The geologic history of seawater—

case except that recent $\delta^{13}C$ are somewhat lower. In each case, it is obvious that $\delta^{13}C$ are negatively correlated with $\delta^{34}S$. Observational data show the same negative correlation. Thus, it is clear that when the organic carbon burial rate increases the pyrite burial rate decreases and inversely, this being possibly linked to the location of organic carbon burial, as suggested by BR. However this assertion does not mean that (16) is reliable, *i.e.* it is possible that the fluctuations of the organic carbon burial rate are not entirely compensated but simply damped by the fluctuations of pyrite burial, so that the atmospheric oxygen production rate could vary. One could consider computing the time evolution of this oxygen production rate with a model of the carbon cycle where observational $\delta^{13}C$ are used as input data as it was the case for $\delta^{34}S$ in our model of the sulfur cycle. SCHIDLOWSKI *et al.* (1977) and SCHIDLOWSKI and JUNGE (1981) have performed similar calculations. However, the validity of this method is not guaranteed when the purpose is the calculation of the evolution of non sulfate-bound oxygen since uncertainties on observational $\delta^{13}C$ are important and actually larger (VEIZER and HOEFS, 1976) than the deviations of observational $\delta^{13}C$ from our calculated values. Another possible reason for which (16) might not be valid is given by LERMAN (1982). If the CO_2 consumed by photosynthesis in reaction R1 is derived from the weathering of $FeCO_3$ instead of $MgCO_3$, then the proportionality factor in Eqn. (16) would be equal to 13/6 instead of 15/8. LERMAN (1982) proposed a more general approach of the problem where the CO_2 source for photosynthesis is the weathering of siderite and dolomite or may even take into account the CO_2 release from the earth's interior by volcanoes.

The results of the S_3 time-dependent model may be used to discuss the history of seawater sulfate. In Fig. 8, the evolution of the ocean sulfate reservoir content is represented for the S_3 time-dependent model which has been previously described (solid line) and for a model in which the gypsum deposition flux is calculated from Eqn. (12') (dashed line). In the latter case, the parameter $S_3(eq)$ was fixed to 19×10^{18} moles. This arbitrary value was chosen midway between $S_3(eq) = 0$ implicit in Eqn. (12) and the present ocean sulfate content, in order to test the sensitivity of the model to kinetics of SO_4^{2-} removal. Initial conditions at 600 my BP and weathering coefficients are the same for the two models and the requirements that the present ocean sulfate reservoir content and present $\delta^{34}S$ of river water be close to the values

$$S_3(0) = 38 \times 10^{18} \text{ moles}$$

$$\delta_R = 8‰$$

are fulfilled in each case. The comparison of Figs. 2 and 8 shows that seawater sulfate concentration is negatively correlated to $\delta^{34}S$, the only effect of setting $S_3(eq)$ to a positive value being to smooth the fluctuations of ocean sulfate. The gypsum deposition flux probably depends on some factors which are not taken into account in Eqns. (12) and (12').

Consequently, the history of ocean sulfate displayed in Fig. 8 remains speculative. However, the negative correlation to $\delta^{34}S$ is obtained with both assumptions on evaporite deposition rate and may be regarded as a significant result. The time variations of S_3 displayed in Fig. 8 are not negligible since departures from the present value of 30% to 40% are obtained. Such departures are small compared to the range of permitted variations between extreme seawater sulfate reservoir content of 2.7×10^{18} moles and 4×10^{20} moles deduced by HOLLAND (1972) from the mineral sequence of evaporites in Phanerozoic sediments.

CONCLUSION

The main purpose of this paper was to analyse the effects of a variation in the present conditions or in various parameters on the past evolution of the sedimentary sulfur cycle.
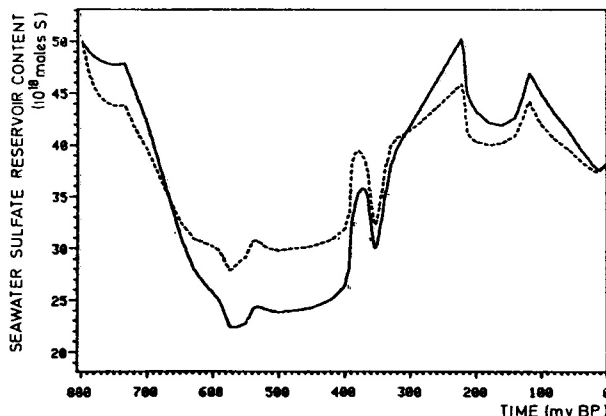

FIG. 8. Evolution of seawater sulfate based on the assumptions that the sulfate deposition flux is related to the ocean sulfate reservoir content through Eqn. (12) (solid line) or (12') (dashed line), with $S_3(eq) = 19 \times 10^{18}$ moles in the latter case. Weathering coefficients are $k_{13} = 0.23 \times 10^{-2}$ my^{-1} and $k_{23} = 0.9 \times 10^{-2}$ my^{-1}.

A model with steady state ocean sulfate has been run. The system of differential equations describing the evolution of the cycle has been integrated backward in time. It is observed that, when the gypsum reservoir content is too low, the integration cannot be pursued until $t = -800$ my. The lack of integrability denotes an incompatibility between the recorded history of the isotopic composition of seawater and a low gypsum reservoir content at the present time. Similarly, a high weathering rate constant k_{23} is not compatible with past $\delta^{34}S$ of ocean sulfate. A new initialization procedure was developed in order to calculate the present state of the cycle. When this method is applied, the size of the domain of integrability may be studied. In general, the integration is favoured by a higher mean $\delta^{34}S$ of the whole sedimentary system ($\bar{\delta}_s$), a more negative fractionation factor $\alpha_s^{(1)}$ during pyrite deposition, higher present reservoir contents or lower fluxes.

The initialization procedure was used to study the sensitivity of the system to the present conditions or to $\bar{\delta}_s$ and $\alpha_s^{(1)}$. It is observed that, when the present reservoir sizes are increased, the evolution curve for this reservoir is simply shifted to higher values. An increase of the present total weathering flux F_{tot} strengthens the fluctuations of the reservoir sizes. A variation of $\bar{\delta}_s$ or $\alpha_s^{(1)}$ has no important consequences on the evolution curves, except for $\alpha_s^{(1)}$ when the initialization procedure is not used. It is also interesting to mention that the evolutions of δ_1 and δ_2—the mean $\delta^{34}S$ of reduced (pyrite) and oxidised (evaporite sulfur) sedimentary reservoir—seem to be well determined except for δ_1 when $\alpha_s^{(1)}$ is varied.

A model with time-dependent ocean sulfate was also developed. It was observed that the problem of integrability vanished, even for low gypsum reservoir contents and a high weathering rate constant k_{23}. Furthermore, the results of this time-dependent model show that the Phanerozoic history of seawater sulfate concentration is negatively correlated to the history of its $\delta^{34}S$. This conclusion is probably only dependent on the assumption that the burial rate of evaporite sulfate increases with the ocean sulfate concentration, as it can be shown with the following arguments. When the ocean sulfate concentration increases, the ratio of the burial rate of evaporite sulfate to the burial rate of pyrite is increased (the pyrite burial rate cannot be increased proportionally to the evaporite sulfate burial rate since, according to BERNER (1984), the rate of bacterial sulfate reduction in seafloor sediments is controlled primarily by the availability and the reactivity of organic matter rather than by the sulfate concentration), so that the mean $\delta^{34}S$ of the sulfur removed from the ocean is higher and seawater sulfate tends to become lighter. Possible departures of 30% to 40% from the present value have been calculated for the evolution of seawater sulfate concentration during the Phanerozoic.

The model presented in this paper is far from complete. Two major approximations have been made. The first one is to consider the sedimentary cycle as closed.

It is clear that, in the real system, metamorphism and volcanism may have affected in an appreciable way the evolution of the sulfur cycle. Secondly, the weathering rate constants k_{13} and k_{23} were assumed constant, although they are dependent on climate (WALKER *et al.*, 1981). The inclusion of this last point would require the calculation of the history of the atmospheric carbon dioxide pressure as well as the exact knowledge of the response of the climate system to an increase in CO_2. An attractive geochemical description of the evolution of the CO_2 cycle has been presented by BERNER *et al.* (1983) and LASAGA *et al.* (1985) for the last 100 million years. However, we feel that many aspects of the calculation of the atmospheric CO_2 pressure in such models remain speculative in view of our present knowledge of the geochemical and atmospheric processes involved. In such a case where the system is not well-known, it is clear that sensitivity studies similar to the one presented here may play a complementary role to improve our understanding of the key processes which govern the evolution of the cycles.

Editorial handling: H. P. Schwarcz

REFERENCES

BERNER R. A. (1984) Sedimentary pyrite formation: an update. *Geochim. Cosmochim. Acta* **48**, 605–615.

BERNER R. A. and RAISWELL R. (1983) Burial of organic carbon and pyrite sulfur in sediments over Phanerozoic time: a new theory. *Geochim. Cosmochim. Acta* **47**, 855–862.

BERNER R. A., LASAGA A. C. and GARRELS R. M. (1983) The carbonate-silicate geochemical cycle and its effect on atmospheric carbon dioxide over the past 100 million years. *Amer. J. Sci.* **283**, 641–683.

BOLIN B., ROSSWALL T., FRENEY J. R., IVANOV M. V., RODHE H. and RICHEY J. E. (1983) C, N, P and S cycles: Major reservoirs and fluxes. In *The Major Biogeochemical Cycles and Their Interactions* (eds. B. BOLIN and R. B. COOK), pp. 41–65. Scope Report No 21, Wiley.

CLAYPOOL G. E., HOLSER W. T., KAPLAN I. R., SAKAI H. and ZAK I. (1980) The age curves of sulfur and oxygen isotopes in marine sulfate and their mutual interpretation. *Chem. Geol.* **28**, 199–260.

DEINES P. and GOLD D. P. (1973) The isotopic composition of carbonatite and kimberlite carbonates and their bearing on the isotopic composition of deep-seated carbon. *Geochim. Cosmochim. Acta* **37**, 1709–1733.

GARRELS R. M. and PERRY E. A. (1974) Cycling of carbon, sulfur and oxygen through geologic time. In *The Sea*, vol. 5, (ed. E. D. GOLDBERG), pp. 303–336. Wiley.

GARRELS R. M. and LERMAN A. (1981) Phanerozoic cycles of sedimentary carbon and sulfur. *Proc. Natl. Acad. Sci. USA* **78**, 4652–4656.

GARRELS R. M. and LERMAN A. (1984) Coupling of the sedimentary sulfur and carbon cycles—an improved model. *Amer. J. Sci.* **284**, 989–1007.

GEAR C. W. (1971) *Numerical Initial Value Problems in Ordinary Differential Equations.* Prentice-Hall, Englewood Cliffs, N.J.

HOLLAND H. D. (1972) The geologic history of seawater—

an attempt to solve the problem. *Geochim. Cosmochim. Acta* **36**, 637–651.

HOLLAND H. D. (1973) Systematics of the isotopic composition of sulfur in the oceans during the Phanerozoic and its implications for atmospheric oxygen. *Geochim. Cosmochim. Acta* **37**, 2605–2616.

HOLLAND H. D. (1978) *The Chemistry of the Atmosphere and Oceans.* Wiley and Sons, 351 p.

HOLSER W. T. and KAPLAN I. R. (1966) Isotope geochemistry of sedimentary sulfates. *Chem. Geol.* **1**, 93–135.

JUNGE C. E., SCHIDLOWSKI M., EICHMANN R. and PIETREK H. (1975) Model calculations for the terrestrial carbon cycle: carbon isotope geochemistry and evolution of photosynthetic oxygen. *J. Geophys. Res.* **80**, 4542–4552.

LASAGA A. C., BERNER R. A. and GARRELS R. M. (1985) An improved geochemical model of atmospheric CO_2 fluctuations over the past 100 million years. In *The Carbon Cycle and Atmospheric CO$_2$: Natural Variations Archean to Present* (eds. E. T. SUNDQUIST and W. S. BROECKER), pp. 397–411. Geophysical Monograph 32, American Geophysical Union.

LERMAN A. (1982) Sedimentary balance through geological time. In *Mineral Deposits and the Evolution of the Biosphere* (eds. H. D. HOLLAND and M. SCHIDLOWSKI) Dahlem Konferenzen, Phys. and Chem. Sci. Res. Rept. no. 3, pp. 237–256. Springer-Verlag.

PISARCHIK Ya. K., GOLUBCHINA M. N. and TOKSUBAYEV A. L. (1977) Isotope ratios of sulfur in calcium sulfate of the Upper Lenskoi Suite of the Siberian Platform. *Geochim. Int.* **14**(2), 182–185.

REES C. E. (1970) The sulfur isotope balance of the ocean: an improved model. *Earth Planet. Sci. Lett.* **7**, 366–370.

SCHIDLOWSKI M. and JUNGE C. E. (1981) Coupling among the terrestrial sulfur, carbon and oxygen cycles: numerical modeling based on revised Phanerozoic carbon isotope record. *Geochim. Cosmochim. Acta* **45**, 589–594.

SCHIDLOWSKI M., JUNGE C. E. and PIETREK H. (1977) Sulfur isotope variations in marine sulfate evaporites and the Phanerozoic oxygen budget. *J. Geophys. Res.* **82**, 2557–2565.

VEIZER J. (1983) Trace elements and isotopes in sedimentary carbonates. In *Carbonates: Mineralogy and Chemistry. Reviews in Mineralogy, Vol. 11* (ed. R. REEDER). Mineralogical Society of America, p. 265.

VEIZER J. and HOEFS J. (1976) The nature of O^{18}/O^{16} and C^{13}/C^{12} secular trends in sedimentary carbonate rocks. *Geochim. Cosmochim. Acta* **40**, 1387–1395.

VEIZER J., HOLSER W. T. and WILGUS C. K. (1980) Correlation of $^{13}C/^{12}C$ and $^{34}S/^{32}S$ secular variations. *Geochim. Cosmochim. Acta* **44**, 579–587.

WALKER J. C. G., HAYS P. B. and KASTING J. F. (1981) A negative feedback mechanism for the long-term stabilization of Earth's surface temperature. *J. Geophys. Res.* **86**, 9776–9782.

APPENDIX

The mathematics of the initialization procedure is described below. This method is used only for the steady state ocean sulfate model, where S_3 is assumed time-independent. Its role is to derive several relations between the present values of the reservoir contents, the isotopic compositions the fluxes and the rate constants. These relations are found from the requirement that the initial values be compatible with the recorded evolution of δ_3, with the differential system and with the present state of the cycle.

Let F_{tot} be the total weathering flux at the present time ($t = 0$), *i.e.*

$$F_{tot} = F_{13} + F_{23} \quad (t = 0). \tag{A1}$$

F_{tot} and $S_1(0)$ are taken as input parameters. It will be seen that, when these two parameters have been assigned a value, the other variables of the model are fixed for time $t = 0$ and initial values are fully determined. The following conditions are imposed at time $t = 0$:

a) the mean $\delta^{34}S$ of river water (δ_R) is equal to 8‰ (PISARCHIK *et al.*, 1977), that is, with approximation (7),

$$\delta_R = \frac{\delta_1 F_{13} + \delta_2 F_{23}}{F_{tot}} = 8‰ \tag{A2}$$

b) the mean $\delta^{34}S$ of the whole system is equal to the primordial value of $\delta^{34}S = 0‰$ (DEINES and GOLD, 1973)

$$\bar{\delta}_S = \frac{\delta_1 S_1 + \delta_2 S_2 + \delta_3 S_3}{S_1 + S_2 + S_3} = 0‰ \tag{A3}$$

c) the ocean sulfate is in steady state

$$F_{13} + F_{23} = F_{31} + F_{32} \tag{A4}$$

d) the system must be compatible with present values of δ_3 and $d\delta_3/dt$ shown in Fig. 2, *i.e.* Eqn. (8″) must be satisfied

$$S_3 \frac{d\delta_3}{dt} = (\delta_1 - \delta_3)F_{13} + (\delta_2 - \delta_3)F_{23} - \alpha_S^{(1)} F_{31} - \alpha_S^{(2)} F_{32}. \tag{A5}$$

The present value of S_3 is the product of the mean sulfate concentration in seawater by the total mass of the oceans, *i.e.* (HOLLAND, 1978)

$$S_3 = 28.2 \times 10^{-3} \text{ (moles/kg)} \times 1.35 \times 10^{21} \text{ (kg)}$$

$$\simeq 38 \times 10^{18} \text{ moles.}$$

From Eqns. (A1) and (A2), comes

$$F_{13} = \frac{\delta_2 - \delta_R}{\delta_2 - \delta_1} F_{tot} \tag{A6}$$

$$F_{23} = \frac{\delta_R - \delta_1}{\delta_2 - \delta_1} F_{tot}. \tag{A6'}$$

Let γ be the present ratio F_{31}/F_{32}, then, using (A1) and (A4), it follows that

$$F_{31} = \frac{\gamma}{1 + \gamma} F_{tot} \tag{A7}$$

$$F_{32} = \frac{1}{1 + \gamma} F_{tot}. \tag{A7'}$$

Combining (A6), (A6'), (A7) and (A7') with (A5) and solving for γ

$$\gamma = \frac{F_{31}}{F_{32}} = \frac{\dfrac{S_3}{F_{tot}} \dfrac{d\delta_3}{dt} - \delta_R + \delta_3 + \alpha_S^{(2)}}{-\dfrac{S_3}{F_{tot}} \dfrac{d\delta_3}{dt} + \delta_R - \delta_3 - \alpha_S^{(1)}}. \tag{A8}$$

Equation (A8) shows that, when the value of F_{tot} is fixed, the ratio $\gamma = F_{31}/F_{32}$ is determined. For example, with GL81's F_{tot} value of 1.5×10^{18} moles/my, $\gamma = 0.498$. Furthermore, for not too small values of F_{tot}, γ cannot be very different from its 0.58 value calculated for $d\delta_3/dt = 0$, because the term $S_3(d\delta_3/dt)/F_{tot}$ is relatively small. It is thus concluded that, for a steady state model, the present ratio F_{31}/F_{32} of pyrite deposition flux to sulfate deposition flux must be close to 0.5. Present mean isotopic compositions of reduced and oxidised sulfur reservoirs are the results of deposition and recycling of pyrite and gypsum during the whole history of the earth, that is (see SCHIDLOWSKI *et al.*, 1977)

$$\delta_1 = \frac{\int_{-\infty}^{0} F_{31}(\tau) e^{k_{13}\tau} (\delta_3(\tau) + \alpha_S^{(1)}) d\tau}{\int_{-\infty}^{0} F_{31}(\tau) e^{k_{13}\tau} d\tau} \tag{A9}$$

$$\delta_2 = \frac{\int_{-\infty}^{0} F_{32}(\tau) e^{k_{23}\tau} (\delta_3(\tau) + \alpha_S^{(2)}) d\tau}{\int_{-\infty}^{0} F_{32}(\tau) e^{k_{23}\tau} d\tau}. \tag{A10}$$

Since recycling times $1/k_{13}$ and $1/k_{23}$ are appreciably less than 800 my, the integrations in (A9) and (A10) may be performed between $t = -800$ my and $t = 0$. In fact, this approximation is of small consequence in view of the uncertainties on $\delta^{34}S$ of evaporite deposits. When S_1 and F_{tot} are fixed, Eqns. (A1), (A2), (A3), (A9) and (A10) combined with (2) and (2') form a system of 7 equations with 7 unknowns S_2, δ_1, δ_2, F_{13}, F_{23}, k_{13} and k_{23}. It can be solved provided the time evolutions of F_{31} and F_{32} are known. An initial guess of these evolutions can be obtained by setting present δ_1 and δ_2 to arbitrary values. The present deposition fluxes $F_{31}(0)$ and $F_{32}(0)$ are found from (A7), (A7') and (A8). Their values are only dependent on F_{tot}, S_3, δ_R and on the evolution of δ_3, which are all fixed quantities. Afterwards, $S_2(0)$, $F_{13}(0)$, $F_{23}(0)$, k_{13} and k_{23} are calculated as the solution of the algebraic system (2), (2'), (A1), (A2) and (A3). When all these initial values are fixed, the differential system is completely determined and its solution gives the time evolution of all the variables in the model. In particular, the method yields the evolution of the deposition fluxes. This calculated function $F_{31}(t)$ is introduced in (A9) and (A10) to derive present δ_1 and δ_2 values compatible with the observed evolution of δ_3. The algebraic system (2), (2'), (A1), (A2) and (A3) is solved again to compute new initial conditions permitting a new integration of the differential system and a new calculation of δ_1 and δ_2. This procedure is repeated until convergence. When the integrability problem mentioned in the text does not appear, this iterative calculation is convergent, so that, when F_{tot} and $S_1(0)$ are fixed, the problem is fully determined.